

## Stress-Induced Shifts of First-Order Raman Frequencies of Diamond- and Zinc-Blende-Type Semiconductors\*

F. Cerdeira, C. J. Buchenauer, Fred H. Pollak, and Manuel Cardona

*Department of Physics, Brown University, Providence, Rhode Island 02912*

(Received 19 July 1971)

In this paper we report measurements of the effects of large static uniaxial stress along [001], [111], and [110] on the frequency of the  $\vec{k} \approx 0$  optical phonons in Ge, GaAs, GaSb, InAs, and ZnSe using first-order Raman scattering. In the absence of stress, the first-order Stokes-Raman spectrum of diamond-type materials exhibits a single peak which corresponds to the  $\vec{k} \approx 0$  triply degenerate optical phonons ( $F_{2g}$  or  $\Gamma_{25'}$ ) while the zinc-blende materials exhibit two peaks, corresponding to the  $\vec{k} \approx 0$  LO and TO phonons. The application of the uniaxial stress causes polarization-dependent splittings and/or shifts which are linear in the stress. From these observed splittings and shifts we have obtained experimental values for the phenomenological coefficients ( $p$ ,  $q$ ,  $r$ ) which describe the changes in the "spring constant" of these optical phonons with strain. Comparison of the experimental values is made with several theoretical considerations based on bond-stretching and bond-bending interactions between atoms. The shift due to the hydrostatic component of the strain yields a value for the mode-Grüneisen parameter, which is compared with the results of hydrostatic-pressure measurements. For the zinc-blende-type materials, the doubly degenerate TO-phonon line exhibits both a splitting and shift with stress, while only a shift is observed for the singlet LO-phonon line. In the case of the III-V compounds, one of the split TO lines has a stress dependence equal to that of the LO-phonon line, while this is not the case for the group II-VI material (ZnSe) we have investigated. This latter result is interpreted in terms of the stress dependence of the effective charge.

### I. INTRODUCTION

During the past few years studies of the effects of uniaxial stress on the optical properties of solids have proven to be extremely useful in understanding the origins of the optical spectra.<sup>1</sup> Although considerable work has been done on the effects of uniaxial stress on the optical properties associated with electronic energy bands, only recently has work been done in the area of vibrational levels. Anastassakis *et al.*<sup>2</sup> have measured uniaxial stress effects on the  $\vec{k} \approx 0$  optical phonons in Si, Harker *et al.*<sup>3</sup> have investigated the stress dependence of the  $A_1$  modes in quartz, and Burke *et al.*<sup>4</sup> have studied stress effects on the lowest two Raman-active modes in SrTiO<sub>3</sub>. In this paper we report measurements on the effects of large static uniaxial stress along [001], [111], and [110] on the frequency of the  $\vec{k} \approx 0$  optical phonons in Ge, GaAs, GaSb, InAs, and ZnSe using first-order Raman scattering.<sup>5</sup> In the absence of stress, the first-order Stokes-Raman spectrum of diamond-type materials exhibits a single peak which corresponds to the  $\vec{k} \approx 0$  triply degenerate optical phonons ( $F_{2g}$  or  $\Gamma_{25'}$ ), while the zinc-blende materials exhibit two peaks, corresponding to the  $\vec{k} \approx 0$  LO and TO phonons. The application of uniaxial stress causes splittings and/or shifts which are linear in the stress. From these observed splittings, the coefficients ( $p$ ,  $q$ ,  $r$ ), which describe the changes in the "spring constant" of the  $\vec{k} \approx 0$  optical phonons with strain, are obtained.

Comparison of the experimental values is made with several theoretical considerations based on bond-stretching and bond-bending interactions between atoms.<sup>6-10</sup> The shift due to the hydrostatic component of the strain yields a value for the mode-Grüneisen parameter, which is compared with the results of hydrostatic-pressure measurements.<sup>11,12</sup>

For the zinc-blende-type materials the nondegenerate LO-phonon line exhibits a shift while both a splitting and a shift is observed for the doubly degenerate TO-phonon line. In the case of the III-V compounds one of the split TO lines has a stress dependence equal to that of the LO-phonon line while this is not the case for the group II-VI material (ZnSe) we have investigated. This latter result is interpreted in terms of the stress dependence of the effective charge.<sup>12</sup>

### II. EXPERIMENTAL DETAILS

The samples used in this experiment were aligned by x-ray diffraction to  $\pm 1^\circ$  and cut into parallelepipeds of dimensions approximately  $20 \times 2 \times 2$  mm. After cutting, the sample faces ( $20 \times 2$  mm) were mechanically polished, chemically etched (CP-4 for the Ge and a dilute solution of bromine in methanol for the zinc-blende-type materials)<sup>13</sup> and mounted in a stress apparatus which has been extensively described in the literature.<sup>1</sup> All samples had room-temperature carrier concentrations of less than  $10^{16}$  cm<sup>-3</sup>. Measurements were made at room temperature in the backscattering configura-

tion using the 4879.9-Å line of a  $\frac{1}{2}$ -W argon-ion laser [Coherent Radiation, model No. 54]. A Jarrell-Ash 1-m double monochromator, with detection by photon counting, was used. The wavelengths of the phonon-shifted lines were determined by comparison with several reference lines of a neon low-pressure lamp. The stress axis was perpendicular to the plane defined by the incident and scattered radiation. The scattering surface was nearly parallel to the entrance slit while the laser beam was kept at an angle of about  $30^\circ$  with the normal to that surface. The sample orientations used are designated as  $x'y'z'$  ([110],  $[\bar{1}10]$ , [001]),  $x''y''z''$  ( $[11\bar{2}]$ ,  $[\bar{1}10]$ , [111]) and  $x'''y'''z'''$  ( $[\bar{1}10]$ , [001],  $[110]$ ). In all cases the stress was applied to the appropriately designated  $z$  axis while the incident and backscattered radiation were along the  $x$  axis. For Ge all three orientations were studied, while for the zinc-blende-type materials only the former two were investigated.

### III. EXPERIMENTAL RESULTS

In the absence of strain the  $\vec{k}=0$  optical phonons in a diamond-type material are triply degenerate ( $F_{2g}$  or  $\Gamma_{25'}$  symmetry) due to the cubic symmetry of the crystal. The application of a uniaxial stress removes this cubic symmetry and hence splits the triplet. In addition there is a shift due to the hydrostatic component of the stress.

In the presence of a strain the dynamical equations for the  $\vec{k}\approx 0$  triply degenerate optical modes

in diamond-type crystals, to terms linear in the strain, has the form<sup>6</sup>

$$\bar{m} \ddot{u}_i = - \sum_k K_{ik} u_k = - \left( K_{ii}^{(0)} u_i + \sum_{klm} \frac{\partial K_{ik}}{\partial \epsilon_{lm}} \epsilon_{lm} u_k \right), \quad (1)$$

where  $u_i$  is the  $i$ th component of the relative displacement of the two atoms in the unit cell;  $\bar{m}$  is the reduced mass of the two atoms;  $K_{ii}^{(0)} = \bar{m} \omega_0^2$  is the effective spring constant of the  $F_{2g}$  modes in the absence of strain;

$$\frac{\partial K_{ik}}{\partial \epsilon_{lm}} \epsilon_{lm} = K_{iklm}^{(1)} \epsilon_{lm} = K_{iklm}^{(1)} \epsilon_{lm}$$

is the change in spring constant due to an applied strain  $\epsilon_{lm}$ ; and  $i, k, l$ , and  $m$  designate  $x$  or  $y$  or  $z$ . From thermodynamic and symmetry considerations it can be shown that for a cubic crystal there are only three independent components of the tensor  $K^{(1)}$ , namely,

$$K_{1111}^{(1)} = K_{2222}^{(1)} = K_{3333}^{(1)} = \bar{m} p,$$

$$K_{1122}^{(1)} = K_{2233}^{(1)} = K_{1133}^{(1)} = \bar{m} q,$$

$$K_{1212}^{(1)} = K_{2323}^{(1)} = \bar{m} r.$$

From Eq. (1) and the above considerations one obtains the following secular equation whose solutions yield the frequencies of the optical phonons in the presence of strain:

$$\begin{vmatrix} p\epsilon_{xx} + q(\epsilon_{yy} + \epsilon_{zz}) - \lambda & 2r\epsilon_{xy} & 2r\epsilon_{xz} \\ 2r\epsilon_{xy} & p\epsilon_{yy} + q(\epsilon_{xx} + \epsilon_{zz}) - \lambda & 2r\epsilon_{yz} \\ 2r\epsilon_{xz} & 2r\epsilon_{yz} & p\epsilon_{zz} + q(\epsilon_{xx} + \epsilon_{yy}) - \lambda \end{vmatrix} = 0, \quad (2)$$

where  $\lambda = \Omega^2 - \omega_0^2$  and  $\Omega \approx \omega_0 + \lambda/2\omega_0$  is the strain-dependent frequency of the optical phonons. The secular equation is referred to the crystallographic axes,  $\hat{x}=[100]$ ,  $\hat{y}=[010]$ , and  $\hat{z}=[001]$ . Diagonalization of Eq. (2) yields the set of three eigenvectors of the optical phonons in the presence of strain.

For uniaxial stress parallel to either the [001] or  $[\bar{1}11]$  directions the threefold degeneracy of the  $\vec{k}\approx 0$  optical phonons is split into a singlet ( $\Omega_s$ ) with eigenvector parallel to the stress and a doublet ( $\Omega_d$ ) with eigenvectors perpendicular to the stress. There is also a shift ( $\Delta\Omega_H$ ) due to the hydrostatic component of the applied stress. For these two stress directions one finds

$$\Omega_s = \omega_0 + \Delta\Omega_H + \frac{2}{3} \Delta\Omega, \quad (3)$$

$$\Omega_d = \omega_0 + \Delta\Omega_H - \frac{1}{3} \Delta\Omega, \quad (4)$$

where  $\omega_0$  is the frequency of the  $\vec{k}\approx 0$  optical phonons

in the absence of stress and

$$\Delta\Omega_H = (X/6\omega_0)(p+2q)(S_{11}+2S_{12}), \quad (5)$$

$$\Delta\Omega = \Omega_s - \Omega_d = \begin{cases} (X/2\omega_0)(p-q)(S_{11}-S_{12}), & X \parallel [001] \\ (X/2\omega_0)rS_{44}, & X \parallel [\bar{1}11]. \end{cases} \quad (6a)$$

$$(6b)$$

In the above equations  $X$  is the applied stress and  $S_{ij}$  are elastic compliance constants referred to the cubic axes.

Since the strain-induced changes in the Raman tensor are relatively small the scattering is, to a good approximation, determined by the first-order Raman scattering tensor of the crystal. In the following discussion we shall use the notation of Loudon<sup>14</sup> [ $F_{2g}(x)$ ,  $F_{2g}(y)$ , and  $F_{2g}(z)$ ] for the Raman tensor. In transforming the Raman tensor to the singly primed axes one finds that the singlet mode

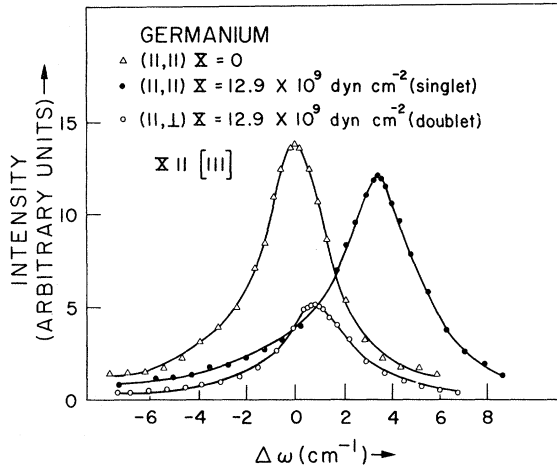


FIG. 1. First-order Stokes-Raman spectrum of Ge for stress  $X=0$  and  $12.9 \times 10^9 \text{ dyn cm}^{-2}$  along the  $[111]$  direction with incident and backscattered radiation along  $[11\bar{2}]$ . The entries in parenthesis designate the polarization direction of the incident and scattered radiation. The zero-stress spectrum peak occurs at  $300.0 \text{ cm}^{-1}$ .

$[F_{2g}(z'')]$  is observed for the  $(\perp, \perp)$  polarization configuration, whereas one of the doublet modes  $[F_{2g}(y'')]$  is observed, with the same intensity, for the  $(\parallel, \perp)$  configuration. Similarly, on transforming to the double primed coordinate axes it is found that the singlet mode  $[F_{2g}(z'')]$  is observed for  $(\parallel, \parallel)$  whereas one of the doublet modes  $[F_{2g}(y'')]$  is observed for  $(\parallel, \perp)$ , with one-fourth the intensity of the singlet.

Shown in Fig. 1 the first-order Stokes-Raman spectrum of Ge corresponding to scattering from the  $\vec{k} \approx 0$  optical phonons for stress  $X=0$  and  $12.9 \times 10^9 \text{ dyn cm}^{-2}$  along the  $[111]$  direction with the incident and backscattered radiation along  $[11\bar{2}]$ . The zero-stress spectrum was measured in the  $(\parallel, \parallel)$  configuration. Application of the uniaxial stress causes the peak to split into two components, the singlet ( $\Omega_s$ ) being observed for the  $(\parallel, \parallel)$  polarization configuration while the doublet ( $\Omega_d$ ) is seen with the  $(\parallel, \perp)$  configuration. The data of Fig. 1 show

TABLE I. Room-temperature elastic compliance constants (in units of  $10^{-12} \text{ dyn}^{-1} \text{ cm}^2$ ) for the materials investigated in this experiment as taken from the compilation in Ref. 7.

	$S_{11}+2S_{12}$	$S_{11}-S_{12}$	$S_{44}$
Si	0.341	0.982	1.26
Ge	0.440	1.24	1.49
GaAs	0.445	1.54	1.69
GaSb	0.591	2.08	2.31
InAs	0.575	2.63	2.53
ZnSe	0.570	3.11	2.27

that for compressive stress along  $[111]$ ,  $\Delta\Omega = \Omega_s - \Omega_d$  is positive. The intensities of the singlet and doublet peaks in Fig. 1 are approximately in the ratio of 4:1, as expected from the first-order selection rules discussed above. Similar results have been obtained in the case of compressive stress along  $[001]$ , except that the sign of  $\Delta\Omega$  is found to be negative.

Curves of  $\Omega_s$  and  $\Omega_d$  as a function of uniaxial stress along  $[111]$  and  $[001]$  for Ge are shown in Fig. 2. The solid and dashed lines represent a linear least-square fit of the data. Using these curves, the elastic compliance constants listed in Table I and Eqs. (3)–(6b) we have obtained the values of  $(p-q)/2\omega_0^2$ ,  $r/\omega_0^2$ , and  $\gamma = -(p+2q)/6\omega_0^2$  listed in Table II. The parameter  $\gamma$  is the mode-Grüneisen parameter and  $\omega_0$  is the frequency of the zero-stress line. Also listed in Table II are the values of these parameters for Si taken from Ref. 2.

For uniaxial stress parallel to  $[110]$  the situation is more complex since the application of the uniaxial stress splits the triply degenerate phonons into three components. For this stress direction Eq. (2) yields

$$\Omega_1 = \omega_0 + \Delta\Omega_H - \frac{1}{3} \Delta\Omega^{(001)}, \quad (7a)$$

$$\Omega_2 = \omega_0 + \Delta\Omega_H + \frac{1}{6} \Delta\Omega^{(001)} + \frac{1}{2} \Delta\Omega^{(111)}, \quad (7b)$$

$$\Omega_3 = \omega_0 + \Delta\Omega_H + \frac{1}{6} \Delta\Omega^{(001)} - \frac{1}{2} \Delta\Omega^{(111)}. \quad (7c)$$

With our geometry it is only possible to observe two ( $\Omega_1$  or  $\Omega_2$ ) of the above modes. Observation of the  $\Omega_3$  mode would be possible by scattering on a face perpendicular to the stress axis. For  $X \parallel [110]$  and a  $[110]$  face, the configuration  $(\parallel, \parallel)$  gives the  $\Omega_1$  mode, while  $(\parallel, \perp)$  gives the  $\Omega_2$  mode. The  $(\perp, \perp)$  configuration is forbidden. For a  $[001]$  face both  $(\parallel, \parallel)$  and  $(\perp, \perp)$  give the  $\Omega_1$  mode, the  $(\parallel, \perp)$  configuration being forbidden. It is thus possible

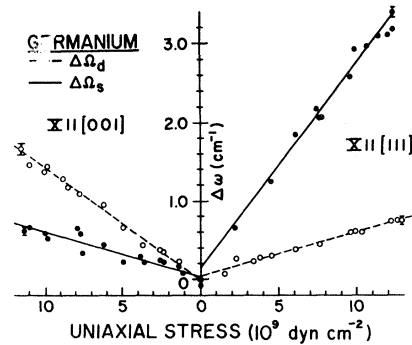


FIG. 2. Stress dependence of the singlet ( $\Omega_s$ ) and doublet ( $\Omega_d$ ) modes of the first-order Raman spectrum of Ge for uniaxial stress along  $[111]$  and  $[001]$ . The solid and dashed lines represent a linear least-squares fit. Representative error bars are shown.

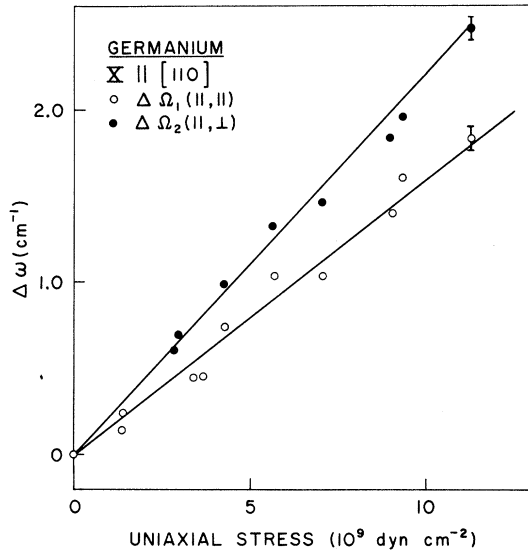


FIG. 3. Stress dependence of the  $\Omega_1$  and  $\Omega_2$  modes of the first-order Raman spectrum of Ge for stress along  $[110]$ . The solid lines represent a fit to Eqs. (7a) and (7b) using the parameters listed in Table II. Representative error bars are shown.

to have an internal check on  $(p-q)$  and  $r$  as obtained from the other stress directions. Shown in Fig. 3 are  $\Omega_1$  and  $\Omega_2$  as a function of uniaxial stress along  $[110]$  for Ge. The solid lines were computed from the parameters obtained for  $[001]$  and  $[111]$  stress.

The polar zinc-blende-type semiconductors have  $T_d$  point symmetry. The Raman-active  $F_{2g}$  modes are still threefold degenerate at  $\vec{k}=0$ . However, they are split by the long-range Coulomb interaction for rather small values of  $|\vec{k}| \gtrsim \omega_0/c$

( $c \equiv$  speed of light in the medium). The change in  $\vec{k}$  involved in backscattering is  $|\Delta\vec{k}| \approx 2\omega_s/c \gg \omega_0/c$ , where  $\omega_s$  is the frequency of the scattering radiation. Thus in the backscattering configuration one should see the full LO-TO splitting produced by the long-range Coulomb potential of the ionic changes. For either  $[001]$  or  $[111]$  stress and with a scattering vector  $\Delta\vec{k}$  perpendicular to the stress the Coulomb interaction and the stress Hamiltonian are simultaneously diagonalized in a set of axes which contains the stress axis and  $\Delta\vec{k}$ . If the LO-TO splitting is small one can assume that it is independent of stress. The behavior of these phonons under stress can be simply obtained by adding the LO-TO splitting to Eqs. (3) and (4) in the appropriate way: One of the doublet components becomes the LO phonon while the singlet and the other doublet component become the TO phonons. We thus obtain

$$\text{LO phonon: } \Omega_s = \omega_{LO} + \Delta\Omega_H - \frac{1}{3}\Delta\Omega, \quad (8a)$$

$$\text{TO phonon: } \begin{cases} \Omega_d = \omega_{TO} + \Delta\Omega_H - \frac{1}{3}\Delta\Omega, & (8b) \\ \Omega_s = \omega_{TO} + \Delta\Omega_H + \frac{2}{3}\Delta\Omega. & (8c) \end{cases}$$

$\Delta\Omega_H$  and  $\Delta\Omega$  are given by Eqs. (5) and (6), with  $\omega_0$  replaced by either  $\omega_{LO}$  or  $\omega_{TO}$ . If the stress dependence of the LO-TO splitting becomes significant we must use in Eqs. (5) and (6) two different sets of values for  $p$ ,  $q$ , and  $r$ , one for the LO phonon and the other for the TO phonons.

For stress parallel to  $[111]$  and a  $[11\bar{2}]$  sample face (which is the geometry used in this experiment for  $[111]$  stress) the LO phonon has symmetry  $F_{2g}(x'')$  while the TO phonons have symmetry  $F_{2g}(y'')$  and  $F_{2g}(z'')$ . Following the notation used for the diamond-type materials we denote  $F_{2g}(z'')$  as the TO (doublet) phonon, while  $F_{2g}(x'')$  and  $F_{2g}(y'')$  become the LO (doublet) and TO (singlet)

TABLE II. Experimental values of the parameters  $(p-q)/2\omega_0^2$ ,  $r/\omega_0^2$ , and  $\gamma = -(p+2q)/6\omega_0^2$  obtained in this experiment (except Si). Listed in parentheses are values of  $\gamma$  determined from hydrostatic-pressure measurements.

	$\omega_0^2$ ( $10^{28} \text{ sec}^{-2}$ )	$\frac{p-q}{2\omega_0^2}$	$\frac{r}{\omega_0^2}$	$\gamma$
Si <sup>a</sup>	0.970	$0.31 \pm 0.06$	$-0.65 \pm 0.13$	$0.90 \pm 0.18$ ( $1.02 \pm 0.02$ ) <sup>b</sup>
Ge	0.319	$0.23 \pm 0.02$	$-10.87 \pm 0.09$	$0.89 \pm 0.09$ ( $1.12 \pm 0.02$ ) <sup>b</sup>
GaAs <sup>c</sup>	0.256	$0.1 \pm 0.1$	$-0.2 \pm 0.2$	$0.90 \pm 0.3$ ( $1.34 \pm 0.08$ ) <sup>b</sup>
GaSb <sup>c</sup>	0.184	$0.22 \pm 0.04$	$-1.08 \pm 0.2$	$1.10 \pm 0.22$ ( $1.23 \pm 0.02$ ) <sup>b</sup>
InAs <sup>c</sup>	0.169	$0.57 \pm 0.12$	$-0.76 \pm 0.15$	$0.85 \pm 0.13$
ZnSe <sup>c</sup>	0.148	$0.62 \pm 0.19$	$-0.43 \pm 0.12$	$1.80 \pm 0.36$ ( $1.7$ ) <sup>d</sup>

<sup>a</sup>Reference 2.

<sup>b</sup>Reference 12.

<sup>c</sup>Refers to measurements on the TO phonon.

<sup>d</sup>Reference 11.

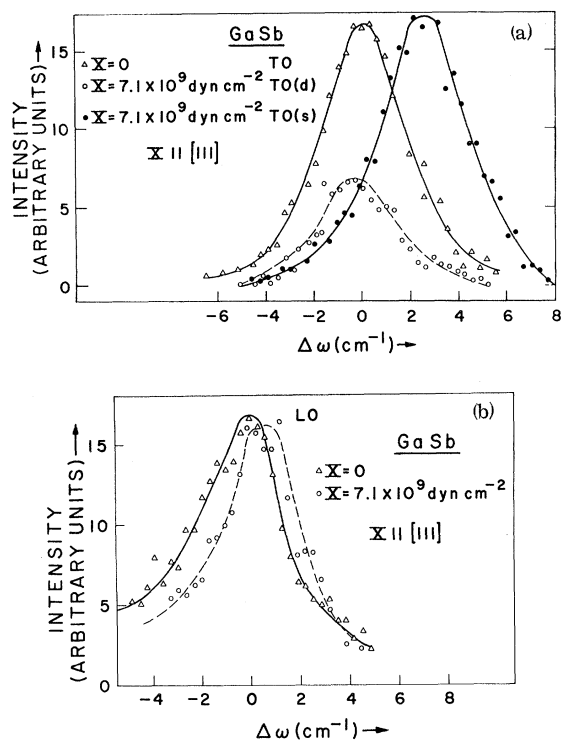


FIG. 4. First-order Stokes-Raman spectrum of GaSb corresponding to scattering from the (a) TO phonons and (b) LO phonons for  $X=0$  and  $7.1 \times 10^9 \text{ dyn cm}^{-2}$  along the  $[111]$  direction with incident and backscattered radiation along  $[11\bar{2}]$ . The TO(s) spectrum was measured in the  $(\perp, \perp)$  polarization configuration, the TO(d) spectrum was obtained from the  $(\parallel, \perp)$  configuration, and the LO spectrum was obtained from the  $(\parallel, \parallel)$  configuration. At zero stress the TO spectrum peak occurs at  $227.5 \text{ cm}^{-1}$  and the LO spectrum peak is observed at  $237.3 \text{ cm}^{-1}$ .

phonons, respectively. Selection rules reveal that for the  $(\perp, \perp)$  configuration both  $F_{2g}(x'')$  and  $F_{2g}(z'')$  are allowed, for  $(\parallel, \perp)$  only  $F_{2g}(y'')$  is allowed, and for  $(\parallel, \parallel)$  only  $F_{2g}(z'')$  is allowed. Since the intensity of  $F_{2g}(z'')$  is a factor of 4 stronger for  $(\parallel, \parallel)$  as compared with  $(\perp, \perp)$  all three polarization configurations were measured for this stress direction.

Shown in Fig. 4(a) is the first-order Raman spectrum of GaSb corresponding to scattering from the TO phonons for  $X=0$  and  $7.1 \times 10^9 \text{ dyn cm}^{-2}$  along the  $[111]$  direction with incident and backscattered radiation along  $[11\bar{2}]$ . The zero of frequency is taken at the position of the peak of the zero-stress spectrum. The application of the stress results in a splitting of the TO-phonon peak into two components, which have been designated TO (s) and TO (d) because they correspond to the singlet and the doublet of the germanium spectrum, respectively. The former spectrum has been measured using the  $(\perp, \perp)$  polarization configuration while the latter has

been obtained from the  $(\parallel, \perp)$  configuration. Plotted in Fig. 4(b) is the first-order Raman spectrum for GaSb corresponding to scattering from the LO phonon for  $X=0$  and  $7.1 \times 10^9 \text{ dyn cm}^{-2}$  along  $[111]$  using the polarization configuration  $(\parallel, \parallel)$ . For the LO phonon only a shift in frequency with stress is observed.

In Figs. 5–8 we have plotted the stress dependence of the TO and LO phonons of GaSb, GaAs, InAs, and ZnSe for  $X \parallel [111]$  and  $X \parallel [001]$ . For  $X \parallel [001]$  with the sample configuration used ( $[1\bar{1}0]$  face) scattering from the LO phonon is not observed. The TO (d) spectrum is allowed only for the configuration  $(\parallel, \perp)$  while TO (s) is allowed only for the  $(\perp, \perp)$  configuration. In this manner we have been able to resolve both of these peaks.

For the III-V compounds (GaSb, GaAs, and InAs) the stress dependence of the LO phonon is equal to that of the TO (d) line (for  $X \parallel [111]$ ) while this is not the case for the group II-VI material (ZnSe) we have investigated. This latter result is probably due to a stress dependence of the effective charge.<sup>12</sup> A difference between the pressure coefficients of the LO and TO phonons in several II-VI materials also has been observed in hydrostatic-pressure measurements.<sup>11,12</sup>

Listed in Table II are the values of  $(p-q)/2\omega_0^2$ ,  $\gamma/\omega_0^2$ , and the mode-Grüneisen parameter  $\gamma = -(p+2q)/6\omega_0^2$  for GaAs, GaSb, InAs, and ZnSe as found from the data of Figs. 5–8 and Eq. (8). For the zinc-blende-type materials, the values of these parameters have been obtained from the stress-induced splittings and shifts of the TO-phonon spectra. We have also listed values of  $\omega_0^2$ , where for the zinc-blende-type materials  $\omega_0$  refers to the zero-stress frequency of the TO phonon. Also listed are values of  $\gamma$  from hydrostatic-pressure

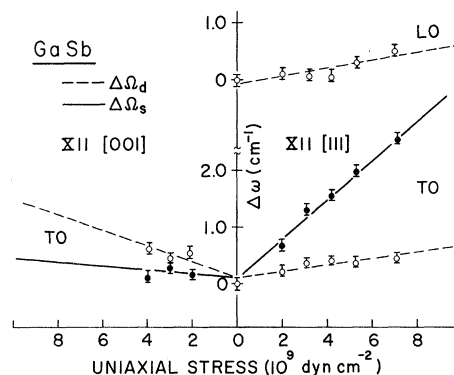


FIG. 5. Stress dependence of the TO and LO phonons in GaSb for stress along the  $[111]$  and  $[001]$  directions. The solid and dashed lines represent a linear least-squares fit. For  $X \parallel [001]$  with the sample configuration used in this experiment ( $[1\bar{1}0]$  face) scattering from the LO phonon is forbidden.

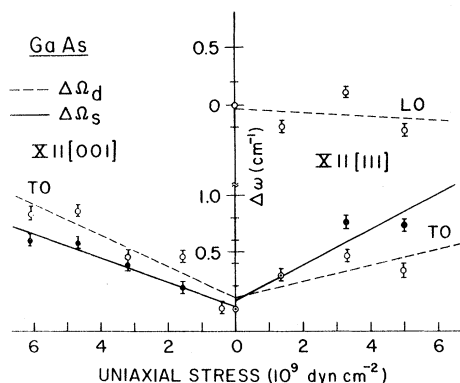


FIG. 6. Stress dependence of the TO and LO phonons in GaAs for stress along the [111] and [001] directions. The solid and dashed lines represent a linear least-squares fit. For  $X \parallel [001]$  with the sample configuration used in this experiment ( $[1\bar{1}0]$ ), face scattering from the LO phonon is forbidden.

measurements.<sup>11,12</sup>

The values of  $\gamma$  obtained from the hydrostatic-pressure experiments are typically 20% larger than those obtained from the uniaxial stress measurement. This result is interpreted as being due to a slight relaxation of the stress applied uniaxially in a surface layer of thickness comparable to the penetration depth of the scattered light. In the case of ZnSe no difference between hydrostatically and uniaxially determined Grüneisen constants exists within the experimental error: The Raman scattering is from the bulk of the material since it is transparent to the incoming and scattered radiation. Differences between hydrostatically and uniaxially determined pressure coefficients have also been

observed for electronic transitions which occur in a region of small absorption.<sup>1</sup> While we do not know the details of the conjectured stress relaxation near the surface, the systematic agreement of the ZnSe results with those of the absorbing materials suggests that any errors due to this effect are of order of 20%. This conclusion has been recently confirmed by reststrahlen measurements in GaAs under uniaxial stress.<sup>15</sup> Since the penetration depth in this region is typically ten times higher than in the visible, stress relaxation effects in this deeper surface layer should be smaller. The Grüneisen parameter so determined agrees better with that found under hydrostatic pressure.

#### IV. THEORETICAL CONSIDERATIONS

A microscopic theory of uniaxial stress effects on  $\bar{k} \approx 0$  optical phonon in materials with the diamond structure was first developed by Ganesan, Maradudin, and Oitmaa.<sup>6</sup> Expressions for the parameters  $p$ ,  $q$ , and  $r$  have been obtained in the quasiharmonic approximation considering only bond-stretching forces between nearest neighbors. Values for these parameters have been estimated using a Morse potential to describe the interaction between neighboring atoms. The signs of  $p$  and  $q$  for Si and Ge which they have obtained are in agreement with our experimental results although there is serious disagreement with regard to the magnitude: The mode-Grüneisen parameter  $\gamma$  which is obtained from their values of  $p$  and  $q$  is a factor of 2 smaller than experimental results. There is also a discrepancy with respect to  $r$ . The sign (negative) and magnitude of  $r$  in Table V of Ref. 6 are incorrect due to an algebraic error on the part of the authors. In

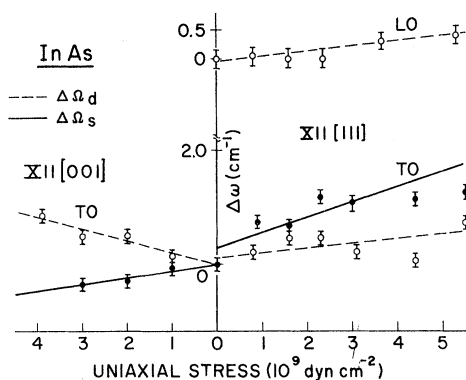


FIG. 7. Stress dependence of the TO and LO phonons in InAs for stress along the [111] and [001] directions. The solid and dashed lines represent a linear least-squares fit. For  $X \parallel [001]$  with the sample configuration used in this experiment ( $[1\bar{1}0]$ ) face scattering from the LO phonon is forbidden.

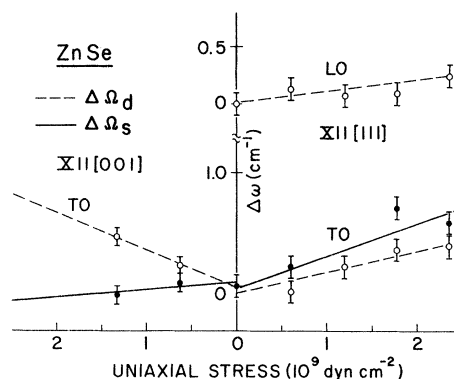


FIG. 8. Stress dependence of the TO and LO phonons in ZnSe for stress along the [111] and [001] directions. The solid and dashed lines represent a linear least-squares fit. For  $X \parallel [001]$  with the sample configuration used in this experiment ( $[1\bar{1}0]$ ) face scattering from the LO phonon is forbidden. In contrast to the other zinc-blende-type materials investigated the stress dependence of the LO phonon is not equal to that of the TO( $d$ ) phonon.

a preprint of this article,<sup>16</sup> which the authors have kindly sent to us, the complete theoretical expression for  $r$  is given in terms of second and third derivatives of the potential (this expression is not given in Ref. 6). An incorrect sign for the second derivative term has caused the above error.

We present in this paper two other models<sup>7,9</sup> to account for the stress-induced splittings and shifts of the  $\tilde{k} \approx 0$  optical phonons. Both of these models contain contributions to the parameters  $p$ ,  $q$ , and  $r$  due to both bond-stretching and bond-bending forces, the latter having been neglected by Ganesan *et al.* In addition third-nearest-neighbor interactions will be included explicitly in the model of Ref. 7.

#### A. Martin's Model

In the following discussion we will first consider the model proposed by Martin<sup>7</sup> and assume that the expansion of the internal energy involves only the squares of the scalar variations  $\Delta(\vec{r}_i \cdot \vec{r}_j)$ , where  $\vec{r}_i$  and  $\vec{r}_j$  are bond vectors about a given atom. The energy can then be written as

$$U = \frac{1}{2} \alpha \left( \frac{3}{4r^2} \right) \sum_{i=1}^4 [\Delta(\vec{r}_i \cdot \vec{r}_i)]^2 + \beta \left( \frac{3}{4r^2} \right) \sum_{i,j>i} [\Delta(\vec{r}_i \cdot \vec{r}_j)]^2 \quad (9a)$$

$$= U_{bs} + U_{bb}, \quad (9b)$$

where  $\alpha$  is the force constant related to the bond-stretching contribution to the energy ( $U_{bs}$ ) and  $\beta$  represents the average of several bond-bending effects and is related to bond-bending contributions to the energy ( $U_{bb}$ ). From the above expression the atomic vibrations will be calculated in the quasi-harmonic approximation. In this approximation the atoms in a crystal subjected to a strain are assumed to execute harmonic vibrations about the new equilibrium positions which are shifted from the equilibrium positions in the absence of the strain. The strain affects the atomic vibrations only through the effective force constants which determine the vibrational frequencies.

In the following analysis the effects of uniaxial stress, both hydrostatic and shear components, along [001] and [111] will be considered. For the hydrostatic component we treat the phonon whose polarization lies along [001] (the result is independent of phonon polarization) while for the shear components we shall consider the phonon whose polarization lies along the direction of the stress, which, by symmetry, is the singlet normal mode of the stressed material. Equations (5) and (6) can then be used to determine  $(p+2q)$ ,  $(p-q)$ , and  $r$  and thus the behavior of the doublet. Since the applied uniaxial stress can be decomposed into hydrostatic and pure-shear components and since these two effects are separable in Eqs. (6) and (8) we

consider them separately.

#### 1. Hydrostatic Pressure

The four bond vectors about a given atom can be written as

$$\begin{aligned} \vec{r}_1 &= \frac{1}{4} a_0 (111), & \vec{r}_2 &= \frac{1}{4} a_0 (-1, -1, 1), \\ \vec{r}_3 &= \frac{1}{4} a_0 (1, -1, -1), & \vec{r}_4 &= \frac{1}{4} a_0 (-1, 1, -1), \end{aligned} \quad (10)$$

where  $a_0$  is the lattice constant.

In the absence of an applied pressure the optical phonon under consideration is a displacement  $(0, 0, z)$  of one of the two sublattices with respect to the other. It can readily be shown that

$$[\Delta(\vec{r}_i \cdot \vec{r}_i)]^2 = \frac{1}{4} a_0^2 z^2 \text{ for } i = 1-4, \quad (11)$$

$$[\Delta(\vec{r}_1 \cdot \vec{r}_2)]^2 = [\Delta(\vec{r}_3 \cdot \vec{r}_4)]^2 = \frac{1}{4} a_0^2 z^2, \quad (12)$$

all other  $\Delta(\vec{r}_i \cdot \vec{r}_j) = 0$ . From Eqs. (9a), (11), and (12) the expression for the energy  $U(0, z)$  in the absence of stress is

$$U(0, z) = 2(\alpha_0 + \beta_0) z^2, \quad (13)$$

where  $\alpha_0$  and  $\beta_0$  are the appropriate bond-stretching and bond-bending force constants in the absence of stress. In general the effective force constant is given by

$$K_{\text{eff}}(\epsilon) = \left. \frac{\partial^2 U(\epsilon, z)}{\partial z^2} \right|_{z=0} \quad (14)$$

and hence

$$K_{\text{eff}}(0) = 4(\alpha_0 + \beta_0). \quad (15)$$

We now consider the effects of a hydrostatic pressure with the strain tensor

$$\vec{\epsilon} = \epsilon \begin{pmatrix} 1 & 0 & 0 \\ 0 & 1 & 0 \\ 0 & 0 & 1 \end{pmatrix}, \quad (16)$$

where  $\epsilon = \frac{1}{3}(S_{11} + 2S_{12})X$ . For  $z = 0$  the above strain produces a change in bond length given by

$$r_i = \frac{1}{4} \sqrt{3} a_0 (1 + \epsilon), \quad i = 1-4. \quad (17)$$

In general  $\alpha$  and  $\beta$  are functions of the interatomic separation, so that they can be expressed as

$$\alpha = \alpha_0 [1 + (n/r_0) \Delta r], \quad (18a)$$

$$\beta = \beta_0 [1 + (m/r_0) \Delta r], \quad (18b)$$

where

$$n = \frac{r}{\alpha} \frac{d\alpha}{dr} \bigg|_{r=r_0} = \frac{d(\ln \alpha)}{d(\ln r)} \bigg|_{r=r_0}, \quad (19a)$$

$$m = \frac{r}{\beta} \frac{d\beta}{dr} \bigg|_{r=r_0} = \frac{d(\ln \beta)}{d(\ln r)} \bigg|_{r=r_0}, \quad (19b)$$

and

$$r_0 = \frac{1}{4} \sqrt{3} a_0. \quad (20)$$

From Eqs. (17) and (20) the strain-induced change in bond length is  $\Delta r = \epsilon r_0$  so that Eqs. (18) become

$$\alpha = \alpha_0(1 + n\epsilon), \quad (21a)$$

$$\beta = \beta_0(1 + m\epsilon). \quad (21b)$$

It can be shown from Eqs. (10) and (16) that when the sublattice displacement is considered

$$\begin{aligned} \sum_{i=1}^4 [\Delta(\vec{r}_i \cdot \vec{r}_i)]^2 &= \sum_{i,j>i} [\Delta(\vec{r}_i \cdot \vec{r}_j)]^2 \\ &= a_0^2(1 + \epsilon)^2 z^2. \end{aligned} \quad (22)$$

Combining the above equations with Eq. (9a) the expression for the energy  $U(\epsilon, z)$  in the presence of the hydrostatic pressure becomes

$$U(\epsilon, z) = 2(\alpha + \beta)z^2 \quad (23)$$

and hence the effective force constant is given by

$$K_{\text{eff}}(\epsilon) = 4(\alpha + \beta). \quad (24)$$

In the harmonic approximation the change in frequency can be written as

$$\begin{aligned} \Delta\omega/\omega_0 &= [K_{\text{eff}}(\epsilon)/K_{\text{eff}}(0)]^{1/2} - 1 \\ &\approx \frac{1}{2} [K_{\text{eff}}(\epsilon) - K_{\text{eff}}(0)]/K_{\text{eff}}(0). \end{aligned} \quad (25)$$

By using Eqs. (15), (24), and (25) the relative change in frequency due to the hydrostatic pressure becomes

$$\Delta\omega/\omega_0 = (n\alpha_0 + m\beta_0)\epsilon/2(\alpha_0 + \beta_0). \quad (26)$$

Comparison of Eqs. (5), (26), and the mode-Grüneisen parameter  $\gamma = -(p + 2q)/6\omega_0^2$  shows that  $\gamma$  is given by

$$\gamma = -(n + \eta_0 m)/6(1 + \eta_0), \quad (27)$$

where

$$\eta_0 = \beta_0/\alpha_0. \quad (28)$$

If it is assumed that the force constants  $\alpha$  and  $\beta$  both scale in the same way with interatomic separation, then  $n = m$  and Eq. (27) yields

$$\gamma = -\frac{1}{6}n. \quad (29)$$

## 2. [001] Stress

In the absence of an applied stress the singlet optical phonon, whose polarization lies along the direction of stress, is the same as that previously considered in the section on hydrostatic pressure. Thus the effective force constant in the absence of stress is given by Eq. (15).

The traceless strain tensor for stress along [001] can be written as

$$\vec{\epsilon} = \epsilon \begin{pmatrix} -1 & 0 & 0 \\ 0 & -1 & 0 \\ 0 & 0 & 2 \end{pmatrix}, \quad (30)$$

where  $\epsilon = \frac{1}{3}(S_{11} - S_{12})X$ . It can be shown that for

$z = 0$  the above strain produces no change in bond length ( $r_i^2 = r_0^2$ ), and hence  $\alpha = \alpha_0$ . There is, however, a change in bond angles, so that

$$\beta = \beta_0(1 + \beta'_0 \Delta\theta_{ij}), \quad (31)$$

where  $\beta'_0 = (1/\beta_0)\partial\beta/\partial\theta$  and  $\theta_{ij}$  is angle between bonds as defined in Ref. 7.

The changes in bond angle with [001] stress are calculated to be  $\Delta\theta_{12} = \Delta\theta_{34} = -4\epsilon/\sqrt{2}$ . As will be shown below these are the only pair of bonds which contribute to the energy  $U_{bb}$  in the presence of stress. If we now allow the sublattice to vibrate with the normalized displacement indicated above, it can be shown that

$$\sum_{i=1}^4 [\Delta(\vec{r}_i \cdot \vec{r}_i)]^2 = (1 + 2\epsilon)^2 z^2 a_0^2 \quad (32)$$

and

$$[\Delta(\vec{r}_1 \cdot \vec{r}_2)]^2 = [\Delta(\vec{r}_3 \cdot \vec{r}_4)]^2 = \frac{1}{4}(1 + 2\epsilon)^2 z^2 a_0^2, \quad (33)$$

all other  $\Delta(\vec{r}_i \cdot \vec{r}_j) = 0$ . With Eqs. (32) and (33) the expression for the energy in the presence of stress [Eq. (9a)] becomes

$$\begin{aligned} U(\epsilon, z) &= 2\alpha_0(1 + 2\epsilon)^2 z^2 + 2\beta(1 + 2\epsilon)^2 z^2 \\ &= 2(\alpha_0 + \beta)(1 + 2\epsilon)^2 z^2. \end{aligned} \quad (34)$$

Thus, the effective force constant in the presence of the strain is given by

$$K_{\text{eff}}(\epsilon) = 4(\alpha_0 + \beta)(1 + 2\epsilon)^2. \quad (35)$$

Combining Eqs. (15), (28), (31), and (35),  $K_{\text{eff}}(\epsilon)$  can be rewritten, to first order in  $\epsilon$ , as

$$K_{\text{eff}}(\epsilon) = K_{\text{eff}}(0) \left( 1 + \frac{1 - \eta_0 \beta'_0}{\sqrt{2}(1 + \eta_0)} 4\epsilon \right). \quad (36)$$

From Eq. (25) the change of frequency of the singlet mode with shear strain, to first order in strain, is given by

$$\frac{\Delta\omega}{\omega_0} = \left( 1 - \frac{\eta_0 \beta'_0}{\sqrt{2}(1 + \eta_0)} \right) 2\epsilon. \quad (37)$$

Comparison of Eqs. (3), (6a), and (37) reveals that the parameter  $(p - q)/2\omega_0^2$  can be written as

$$\frac{(p - q)}{2\omega_0^2} = 1 - \frac{\eta_0 \beta'_0}{\sqrt{2}(1 + \eta_0)}. \quad (38)$$

Equation (38) can be compared to the results obtained by Ganesan and co-workers<sup>6,16</sup> if the term in  $\beta'_0$  is neglected, since they only considered bond-stretching contribution to the parameters. As mentioned before, theoretical expressions for  $p$  and  $q$ , in terms of second and third derivatives of the interaction potential, are presented in the preprint of Ref. 6 but have not been included in the publication. These authors find that

$$p - q = (16/3M)\Phi''(r_0),$$

where  $M$  is the mass of the atom and  $\Phi''(r_0)$  is the



second derivative of the potential evaluated at the equilibrium position  $r_0$ . From Eqs. (12), (13a), and (22) of Ref. 6, for  $X \parallel [001]$ , it can be shown that

$$(8/3M)\Phi''(r_0) = \omega_0^2,$$

where  $\omega_0$  is the zero-stress Raman frequency. Thus, the above expression for  $(p - q)$  becomes

$$(p - q) = 2\omega_0^2,$$

which agrees with Eq. (38) if the term in  $\beta'_\theta$  is neglected. We find, however, that there are discrepancies between the above relations and the numerical values for these parameters given in Ref. 6. For example, the values of  $\Phi''(r_0)$  listed in Table I for Ge and Si, when inserted into the above expression yields a value of  $\omega_0^2$  which is approximately a factor of 2 smaller than experimental value. However, the ratio of  $\Phi''(r_0)$  for these two materials is in good agreement with the ratio of the experimental numbers. Similar consideration apply for  $(p - q)$ . Since these authors have not indicated in sufficient detail the manner in which  $\Phi''(r_0)$  has been evaluated, we are unable to determine the source of the discrepancy.

### 3. $[111]$ Stress

For this direction of stress the situation is somewhat more complicated than for  $[001]$  stress since the microscopic strain is not sufficient to characterize the strained crystal: We must also take into consideration an internal strain within the unit cell.<sup>17</sup> For  $X \parallel [111]$  the traceless macroscopic strain tensor can be written as

$$\epsilon = \epsilon \begin{pmatrix} 0 & 1 & 1 \\ 1 & 0 & 1 \\ 1 & 1 & 0 \end{pmatrix}, \quad (39)$$

where  $\epsilon = \frac{1}{6} S_{44} X$ .

In Fig. 9 we show an atom and its four nearest neighbors in a crystal strained in the  $[111]$  direction as given by Eq. (39). If the atom remains at the center of the strained cube the  $[111]$  bond is of length  $\frac{1}{4}\sqrt{3}a_0(1+2\epsilon)$  and the other three bonds are of length  $\frac{1}{4}\sqrt{3}a_0(1-\frac{2}{3}\epsilon)$ . In this case the internal strain parameter  $\zeta=0$  and the interlattice vector is determined by the microscopic strain tensor. If we allow the central atom to move according to the macroscopic strain displacement vector  $(\frac{1}{2}a_0)(\epsilon, \epsilon, \epsilon)$  all four bonds attain their unstrained length of  $\frac{1}{4}\sqrt{3}a_0$ ; this situation is achieved when  $\zeta=1$ . The internal strain parameter  $\zeta$  is equal to 0.546 for Ge and 0.557 for Si.<sup>7</sup> It should increase with increasing ionicity.<sup>7</sup>

Following the procedure used in the previous sections we first determine the effective force constant on the central atom for a normalized displacement  $(1/\sqrt{3})(z, z, z)$  in the absence of stress.

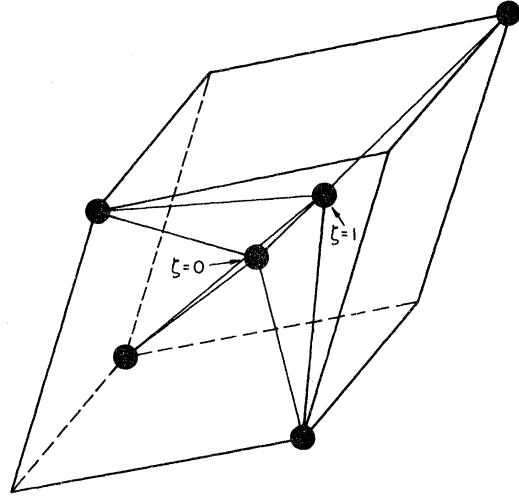


FIG. 9. Deformed unit cell of a diamond-type lattice under a traceless  $[111]$  strain [Eq. (39)] for  $\zeta=0$  and  $\zeta=1$ .

Symmetry considerations show that  $K_{\text{eff}}(0)$  is the same as Eq. (15).

We now take into account the effects of the strain of Eq. (39) and the internal strain parameter  $\zeta$ . The vectors from the central atom to its four nearest neighbors are:

$$\vec{r}_1 = \frac{1}{4}a_0(1+2\sigma, 1+2\sigma, 1+2\sigma), \quad (40a)$$

$$\vec{r}_2 = \frac{1}{4}a_0(-1-2\epsilon\zeta, -1-2\epsilon\zeta, 1-2\epsilon-2\epsilon\zeta), \quad (40b)$$

$$\vec{r}_3 = \frac{1}{4}a_0(1-2\epsilon-2\epsilon\zeta, -1-2\epsilon\zeta, -1-2\epsilon\zeta), \quad (40c)$$

$$\vec{r}_4 = \frac{1}{4}a_0(-1-2\epsilon\zeta, 1-2\epsilon-2\epsilon\zeta, -1-2\epsilon\zeta), \quad (40d)$$

where  $\sigma = \epsilon(1-\zeta)$ . It can be seen from the above equations that if  $\zeta=0$ ,  $|\vec{r}_1| = (\frac{1}{4}\sqrt{3}a_0)(1+2\epsilon)$ ,  $|\vec{r}_2| = |\vec{r}_3| = |\vec{r}_4| = (\frac{1}{4}\sqrt{3}a_0)(1-\frac{2}{3}\epsilon)$ , while if  $\zeta=1$  all four vectors have magnitude  $\frac{1}{4}\sqrt{3}a_0$ , in agreement with the discussion of the internal strain parameter  $\zeta$  given above.

Since for this stress direction there is, in general, a change in bond length and this change is different for  $\vec{r}_1$  and the three other bond vectors, we write

$$\alpha_i = \alpha_0(1+n\Delta r_i/r_0), \quad i=1-4. \quad (41)$$

From the above considerations we find that

$$\alpha_1 = \alpha_0(1+2n\sigma), \quad (42a)$$

$$\alpha_{2,3,4} = \alpha_0(1-\frac{2}{3}n\sigma). \quad (42b)$$

The contribution of the bond stretching to the energy of Eq. (6a) is then given by

$$U_{\text{bs}}(\epsilon, z) = 2\alpha_0[1+4\epsilon f(n, \zeta)]z^2, \quad (43a)$$

where

$$f(n, \zeta) = \frac{1}{3}[n(1 - \zeta) + 2\zeta + 1] \quad (43b)$$

With regard to the bond-bending contribution to  $U$  there will be contributions to the parameter  $\beta$  from both a change in angle, as in the case of [001] stress, and the change due to the bond length. We can thus write

$$\beta_{ij} = \beta_0(1 + \beta'_\theta \Delta\theta_{ij} + \beta' \Delta R_{ij}), \quad (44)$$

where

$$R_{ij} = [|\vec{r}_i| |\vec{r}_j|]^{1/2}$$

and

$$\beta' = \frac{1}{\beta_0} \frac{\partial \beta}{\partial R}.$$

It can be shown that the bond-bending terms are grouped into two categories: The terms with indices 12, 13, and 14 giving one contribution and the terms with indices 23, 24, and 34 giving another. The quantities  $\Delta\theta$  and  $\Delta R$  are calculated to be

$$\Delta\theta_{12} = -\Delta\theta_{23} = 4\epsilon(1 + 2\zeta)/3\sqrt{2} \quad (45a)$$

and

$$\Delta R_{12} = -\Delta R_{23} = \frac{2}{3} r_0 \sigma, \quad (45b)$$

and hence Eq. (44) can be rewritten as

$$\beta_{12} = \beta_0(1 + \delta), \quad (46a)$$

$$\beta_{23} = \beta_0(1 - \delta), \quad (46b)$$

where

$$\delta = \beta'_\theta \Delta\theta + \beta' \Delta R.$$

The terms  $[\Delta(\vec{r}_i \cdot \vec{r}_j)]^2 / R_{ij}^2$  have also been calculated with the result that

$$[\Delta(\vec{r}_1 \cdot \vec{r}_2)]^2 / R_{12}^2 = \frac{4}{9} [1 + \frac{8}{3} \epsilon(1 - 4\zeta)] \quad (47a)$$

and

$$[\Delta(\vec{r}_2 \cdot \vec{r}_3)]^2 / R_{23}^2 = \frac{4}{9} [1 + \frac{8}{3} \epsilon(2 + 4\zeta)]. \quad (47b)$$

The above equations can then be combined to give the total contribution to the bond-bending portion of the total energy  $U_{bb}(\epsilon, z)$

$$U_{bb}(\epsilon, z) = \{\beta_{12} [1 + \frac{8}{3} \epsilon(1 - 4\zeta)] + \beta_{23} [1 + \frac{8}{3} \epsilon(2 + 4\zeta)]\} z^2 \quad (48a)$$

$$= 2\beta_0(1 + 4\epsilon)z^2. \quad (48b)$$

From Eqs. (43a) and (48b) the total energy in the presence of a [111] stress is

$$U(\epsilon, z) = 2\alpha_0 \{1 + \eta_0 + 4\epsilon[\eta_0 + f(n, \zeta)]\} z^2. \quad (49)$$

In a manner similar to that used in the previous section the relative shift in frequency is found to be, to first order in the strain,

$$\Delta\omega/\omega_0 = 2\epsilon[\eta_0 + f(n, \zeta)]/(1 + \eta_0). \quad (50)$$

Comparing Eqs. (5), (6b), and (50) we find

$$\frac{r}{\omega_0^2} = \frac{\eta_0 + f(n, \zeta)}{1 + \eta_0}. \quad (51)$$

Having derived the theoretical expressions for the parameters  $(p - q)/2\omega_0^2$  [Eq. (38)] and  $r/\omega_0^2$  [Eq. (51)] it is possible to compare them with the experimental results listed in Table II.

Consider first the case of [001] stress. The results of Section IV A 2 show that the first term in Eq. (38), which is unity, comes from bond stretching while the second term comes from the bond-bending contribution. Table II shows that for all the materials measured  $(p - q)/2\omega_0^2$  is less than unity. We will now examine the second term in Eq. (38) and show that it is not large enough and probably has the wrong sign to account for the above-mentioned difference in  $(p - q)/2\omega_0^2$  so that other effects have to be taken into account. The logarithmic decrement of  $\beta$  with respect to bond angle is given by  $\theta\beta'_\theta$ , where  $\theta$  is the bond angle ( $\approx 1.9$ ). We might expect the change in  $\beta$  with respect to angle to be at least a factor of 3 smaller than the change in  $\beta$  with bond length, since a change in angle alters only one of the three bond lengths in the three-body interaction associated with the bond-bending term. From Sec. IV A 1 we have that  $m$ , the logarithmic decrement of  $\beta$  with respect to bond length, equals  $-6\gamma$  ( $\approx -7$  for Ge or Si). Hence  $|\theta\beta'_\theta| \approx \frac{7}{3} = 2.3$  and  $|\beta'_\theta| \approx 1.2$ . Also, we might expect  $\beta'_\theta$  to be negative since a decrease in the bond angle  $\theta$  should cause  $\beta$  to increase. We therefore conclude that the sign and magnitude of  $\beta'_\theta$  are not appropriate to account for the discrepancy between Eq. (38) and the observed values of  $(p - q)/2\omega_0^2$ . Considerations of the bond-stretching contribution of third neighbors will considerably improve the agreement.

In the case of [111] stress all of the measured values of  $r/\omega_0^2$  are negative [see Table II]. Equations (43b) and (51) show that the only source of a negative contribution to this parameter comes from the bond-stretching term  $f(n, \zeta)$  and that this term is very sensitive to the value of  $\zeta$ . In Fig. 10 we have plotted  $f(n, \zeta)$  as a function of  $\zeta$  for  $n = -6$ , which would be the case for Si with  $\gamma \approx 1.0$ . In order to account for the experimental value of  $r/\omega_0^2 = -0.65$  in Si ( $\eta_0 = 0.285$ ), Eq. (51) shows that  $f(n, \zeta) = -1.12$  and hence  $\zeta = 0.21$ . This value of  $\zeta$  is considerably smaller than that measured experimentally<sup>18</sup> or deduced by Martin from measurements of elastic constants.<sup>7</sup> Similar difficulties with the value of  $\zeta$  occur for the other materials we have measured. The problem arises because of the cancellation between the bond-stretching and bond-bending contributions to  $r/\omega_0^2$ , as indicated in Eq. (51). In contrast to the situation for [001] stress, it will be shown that considerations of third-nearest-neighbor bond-stretching interactions are not sufficient to account for the above discrepancies.

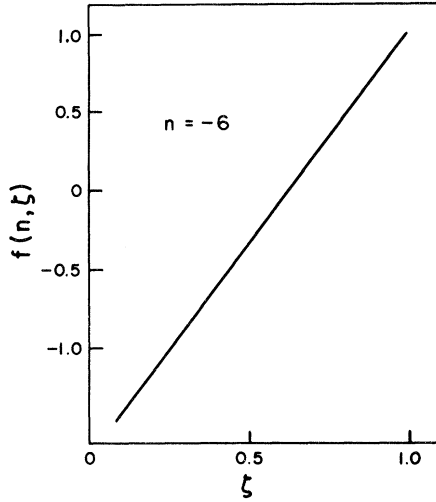


FIG. 10. Function  $f(n, \zeta)$  [see Eq. (43b)] vs  $\zeta$  for  $n = -6$ .

#### 4. Third-Nearest-Neighbor Interaction

In the Appendix we have listed the third-nearest-neighbor bond vectors. In a manner similar to that used in the previous sections, it can be shown that the contribution of the third-nearest-neighbor interaction to the bond-stretching energy in the case of  $X_{II}$  [001] is given by

$$U(0, z) = 6\alpha'_0 z^2, \quad (52)$$

$$U(\epsilon, z) = 6\alpha'_0 [1 + 4\epsilon g(n)] z^2, \quad (53)$$

where  $\alpha'_0$  is the bond-stretching force constant associated with the third-nearest-neighbor interaction. From Eqs. (14), (33), (52), and (53), neglecting  $\beta'_\theta$ , we find that

$$K_{\text{eff}}(0) = 4(\alpha_0 + \beta_0 + 3\alpha'_0), \quad (54)$$

$$K_{\text{eff}}(\epsilon) = 4\{(\alpha_0 + \beta_0)(1 + 4\epsilon) + 3\alpha'_0[1 + 4\epsilon g(n)]\}, \quad (55)$$

and hence from Eq. (22) and (6a) we have

$$\frac{p-q}{2\omega_0^2} = \frac{\alpha_0 + \beta_0 + 3\alpha'_0 g(n)}{\alpha_0 + \beta_0 + 3\alpha'_0} \quad (56a)$$

$$= \frac{1 + \eta_0 + 3\eta'_0 g(n)}{1 + \eta_0 + 3\eta'_0}, \quad (56b)$$

where

$$\eta'_0 = \alpha'_0 / \alpha_0 \quad (57)$$

and

$$g(n) = 1 + \frac{1}{2} \left( \frac{8}{11} \right)^2 (n-2). \quad (58)$$

In the case of Si with  $\eta_0 = 0.285$ ,  $n = -6$ , and  $(p-q)/2\omega_0^2 = 0.31$ , Eq. (56a) yields a value of  $\eta'_0 = 0.24$ , which seems quite reasonable. For ZnSe, which is the most ionic materials we have

measured  $\gamma = 1.70$ ,  $n = -10.2$ ,  $\eta_0 = 0.120$ , and  $(p-q)/2\omega_0^2 = 0.62$ , and hence Eq. (56b) gives a value of  $\eta'_0 = 0.05$ . It is expected that as the material becomes more ionic the third-nearest-neighbor interaction should become considerably weaker in relation to the nearest-neighbor forces.

For  $X_{II}$  [111],  $U(\epsilon, z)$  due to the third-nearest-neighbor bond-stretching interaction is given by (see the Appendix)

$$U(\epsilon, z) = 6\alpha'_0 [1 + 4\epsilon h(n, \zeta)] z^2, \quad (59)$$

where

$$h(n, \zeta) = 1 + \frac{(n-2)(19-9\zeta)}{(11)^2}. \quad (60)$$

$U(0, z)$  is given by Eq. (52). Combining Eqs. (43a), (48b), and (59) and proceeding in a manner similar to that used in Sec. IVA 2, we find that

$$\frac{r}{\omega_0^2} = \frac{\eta_0 + f(n, \zeta) + 3\eta'_0 h(n, \zeta)}{1 + \eta_0 + 3\eta'_0}. \quad (61)$$

For all the materials we have investigated it can be demonstrated that the magnitude of  $\eta'_0 h(n, \zeta)$  is too small to substantially effect the cancellation discussed above. For example, in Si ( $n = -6$ ,  $\zeta = 0.556$ )  $h = 0.07$  and since  $\eta'_0 = 0.24$ , the third-neighbor contribution to  $r/\omega_0^2$  is extremely small.

In Sec. IVA 3 we have attempted to account for the observed values of the parameters  $(p-q)/2\omega_0^2$ ,  $r/\omega_0^2$ , and  $\gamma$  by means of the Martin model [Eq. (9a)], which includes two-body bond-stretching and an average three-body bond-bending interaction. It was found that this formulation did not adequately account for the above shear parameters and that in the case of [001] stress better agreement could be achieved by considering bond-stretching interactions between third nearest neighbors. For [111] stress this approach did not prove fruitful.

#### B. Generalized Force Constant Model

Another approach to the problem would be to express the internal energy as a function of generalized force constants which include two-, three-, and four-body interactions.<sup>8-10</sup> This model has been used by several authors to fit the phonon dispersion curves for several diamond- and zinc-blende-type materials.<sup>9,10,14,19,20</sup> In this model the internal energy per unit cell is written as

$$\begin{aligned} U = & \frac{1}{2} \sum_{i=1}^4 K_i^i (\Delta r_i)^2 + \sum_{i,j>i}^4 K_{ij}^{ij} r_i r_j (\Delta \theta_{ij})^2 \\ & + \sum_{i,j>i}^4 K_{r\theta}^{ij} (r_i r_j)^{1/2} (\Delta \theta_{ij}) (\Delta r_i) + \sum_{i,j>i}^4 K_{rr}^{ij} (\Delta r_i) (\Delta r_j) \\ & + \sum K_{\theta\theta}^{ijk} r_j (r_i r_k)^{1/2} (\Delta \theta_{ij}) (\Delta \theta_{jk}) \\ & + \sum * K_{\theta\theta}^{ijk} r_j (r_i r_k)^{1/2} (\Delta \theta_{ij}) (\Delta \theta_{jk}), \quad (62) \end{aligned}$$

where

$$\Delta r_i = |\vec{r}_i(\epsilon, z)| - |\vec{r}_i(\epsilon, 0)|, \quad (63a)$$

$$\Delta \theta_{ij} = \theta_{ij}(\epsilon, z) - \theta_{ij}(\epsilon, 0). \quad (63b)$$

In addition to two- ( $K_r$ ) and three- ( $K_\theta$ ,  $K_{r\theta}$ ,  $K_{rr}$ ) body force constants, which is somewhat similar to the formulation of Eq. (9a), the four-body force constants ( $K_{\theta\theta}$  and  $*K_{\theta\theta}$ ) have been explicitly introduced. References 8 and 9 give an excellent discussion of the physical significance of the six force constants mentioned above. In particular  $K_{\theta\theta}$  is related to changes in two angles which have a common leg and apex while  $*K_{\theta\theta}$  is related to changes in two angles which have all legs coplanar.

As in Sec. IV A 4 in order to determine the influence of a hydrostatic pressure, with strain tensor given by Eq. (15), we consider a sublattice displacement (0, 0,  $z$ ). It can be shown that in the presence of the above strain the quantities of  $\Delta r$  and  $\Delta \theta$  are given by

$$\Delta r_1 = \Delta r_2 = \epsilon r_0 - z/\sqrt{3}, \quad (64a)$$

$$\Delta r_3 = \Delta r_4 = \epsilon r_0 + z/\sqrt{3}, \quad (64b)$$

$$\Delta \theta_{12} = -\Delta \theta_{34} = \left(\frac{8}{3}\right)^{1/2}(1 - \epsilon)z/r_0, \quad (64c)$$

all other  $\Delta \theta_{ij} = 0$ . Combining Eqs. (62), (64), and (11) the expression for the effective spring constant  $K_{\text{eff}}$ , can then be written as

$$K_{\text{eff}}(\epsilon) = \frac{4}{3}K_r + \frac{32}{3}K_\theta - \frac{32}{3}\sqrt{2}K_{r\theta} - \frac{8}{3}K_{rr} + \frac{64}{3}*K_{\theta\theta}. \quad (65)$$

From Eqs. (3), (15), and (22) and since for hydrostatic pressure  $3\epsilon = dV/V = d \ln V = 3d \ln r$ , where  $V$  is the volume,

$$\gamma = -\frac{p+2q}{6\omega_0^2} = -\frac{1}{6} \frac{d \ln K_{\text{eff}}}{d \ln r}. \quad (66)$$

If we now assume, as has been done in Sec. IV A 4 on hydrostatic pressure, that all the force constants scale in the same way with interatomic distance, i. e.,  $K_{\alpha\beta} = K_{\alpha\beta}^0(r/r_0)^n$  then Eq. (66) with Eq. (65) becomes

$$\gamma = -\frac{1}{6}n, \quad (67)$$

which is the same as Eq. (29).

### 1. [001] Stress

For the case of [001] stress, with strain tensor given by Eq. (30) and the displacement (0, 0,  $z$ ) the parameters of Eqs. (63) are given by

$$\Delta r_1 = \Delta r_2 = -\Delta r_3 = -\Delta r_4 = -\frac{1}{3}\sqrt{3}(1+2\epsilon)z, \quad (68a)$$

$$\Delta \theta_{12} = -2\sqrt{2}\epsilon + \left(\frac{8}{3}\right)^{1/2}(1 - \epsilon)z/r_0, \quad (68b)$$

$$\Delta \theta_{34} = -2\sqrt{2}\epsilon - \left(\frac{8}{3}\right)^{1/2}(1 - \epsilon)z/r_0, \quad (68c)$$

all other  $\Delta \theta_{ij} = 0$ . Since for this stress direction the bond length does not change with stress any stress dependence of the generalized force con-

stants can only depend on  $\Delta \theta$  [such as that given in Eq. (31)]. However, we have presented arguments in Sec. IV A 2 to indicate that this dependence is small and hence we will also neglect it in this case. Equations (13), (62), and (68) then yield, to first order in the strain,

$$K_{\text{eff}}(\epsilon) = \frac{2}{3}K_r^0(1+4\epsilon) + \frac{16}{3}K_\theta^0(1-2\epsilon) - \frac{16}{3}\sqrt{2}K_{r\theta}^0(1+\epsilon) - \frac{4}{3}K_{rr}^0(1+4\epsilon) + \frac{32}{3}*K_{\theta\theta}^0(1-2\epsilon). \quad (69)$$

Combining Eqs. (6a), (22), and (69), we find

$$\frac{p-q}{2\omega_0^2} = \frac{K_r^0 - 4K_\theta^0 - 2\sqrt{2}K_{r\theta}^0 - 2K_{rr}^0 - 8*K_{\theta\theta}^0}{K_r^0 + 8K_\theta^0 - 8\sqrt{2}K_{r\theta}^0 - 2K_{rr}^0 + 16*K_{\theta\theta}^0}. \quad (70)$$

Complete experimental values for the generalized force constants of Eq. (62) for silicon have been determined by Solbrig.<sup>10</sup> Inserting these values into Eq. (70) yields a value of  $(p-q)/2\omega_0^2 = 0.57$ . Although this value is still larger than the experimental value listed in Table II, the agreement is considerably better than that predicted by Eq. (38), neglecting the term in  $\beta'_\theta$ .

### 2. [111] Stress

For this stress direction, in contrast to the case of [001] stress, there is a change in bond length as well as bond angle. Therefore, in order to use the model of Eq. (62) six new parameters, associated with the changes of the  $K_{\alpha\beta}^{ijk}$  with bond length, would have to be introduced. This large number of undetermined parameters makes the use of this model for this stress direction prohibitive.

## V. CONCLUSIONS

The stress dependence of the first-order Raman spectra associated with the  $\vec{k} \approx 0$  optical phonons in Si, Ge, GaAs, GaSb, InAs, and ZnSe has enabled us to determine values for the phenomenological coefficients which describe the changes in the "spring constant" of these optical phonons with strain. Comparison of these experimental values with several theoretical models indicates that none of them are completely satisfactory. The simple bond-stretching model (with implicit contributions of bond bending through the parameter  $\zeta$ ) gives a reasonable fit to the experimental data and indicates the origins of the ionicity trends. The improved agreement in  $(p-q)/2\omega_0^2$  when third-nearest-neighbor interactions were included indicates that long-range forces play an important role for this parameter while they proved unimportant for the description of  $r$ . Explicit inclusion of an average bond-bending force as proposed by Martin reduces the agreement with experiment, particular for  $r$ . This might be an indication that this average bond-bending force is not detailed enough to account for anharmonic coefficients such as  $p$ ,  $q$ , and  $r$ .

## APPENDIX: THIRD-NEAREST-NEIGHBOR CONTRIBUTIONS

We shall compute here third-neighbor contribution to the parameters  $p$ ,  $q$  and  $r$  taking only into account bond-stretching forces. The third-nearest-neighbor bond vectors are

$$\begin{aligned}\vec{r}_1 &= (\tfrac{1}{4}a_0)(1, 1, 3), & \vec{r}_7 &= (\tfrac{1}{4}a_0)(1, -1, 3), \\ \vec{r}_2 &= (\tfrac{1}{4}a_0)(-1, -1, 3), & \vec{r}_8 &= (\tfrac{1}{4}a_0)(-1, 1, -3), \\ \vec{r}_3 &= (\tfrac{1}{4}a_0)(3, 1, 1), & \vec{r}_9 &= (\tfrac{1}{4}a_0)(3, -1, -1), \\ & & & (A1) \\ \vec{r}_4 &= (\tfrac{1}{4}a_0)(-3, -1, 1), & \vec{r}_{10} &= (\tfrac{1}{4}a_0)(-3, 1, -1), \\ \vec{r}_5 &= (\tfrac{1}{4}a_0)(1, 3, 1), & \vec{r}_{11} &= (\tfrac{1}{4}a_0)(1, -3, -1), \\ \vec{r}_6 &= (\tfrac{1}{4}a_0)(-1, -3, 1), & \vec{r}_{12} &= (\tfrac{1}{4}a_0)(-1, 3, -1).\end{aligned}$$

The length of the  $i$ th bond is given by

$$r_i^2 = r_0^2 = \tfrac{1}{4} \sqrt{11} a_0.$$

To compute the bond-stretching contribution to the restoring force we take an approach which simplifies our calculations and is entirely equivalent to the use of Martin's formula [Eq. (9a)] with  $\beta = 0$ . We first notice that the restoring force along the direction of the stress is given by

$$F = \sum_i 3z\alpha'_i \cos^2\theta_i, \quad (A2)$$

where  $z$  is the displacement produced by a vibration along the stress axis (singlet mode),  $\alpha'_i$  is the parameter  $\alpha'$  for the  $i$ th atom, and  $\theta_i$  is the angle between  $\vec{r}_i$  and the stress axis. Here the number 3 in Eq. (A2) is taken so that the definition of  $\alpha$  for this approach coincides with that of Eq. (9a), and the prime on  $\alpha$  indicates that the force constant for first and third neighbors is not the same. From Eq. (A2) we observe that when computing the total restoring force all bonds that have the same projection on the stress axis (in absolute value) give the same contribution to the effective force constant. This reduces considerably the number of bonds to be taken into account for each specific case.

## 1. [001] Stress

In the unstrained crystal only two bonds need be considered:

$$(r_1) \cos^2\theta_1 = \tfrac{9}{11}, \quad (r_2) \cos^2\theta_2 = \tfrac{1}{11}. \quad (A3)$$

Using Eqs. (A2) and (A3) we find for the third neighbor contribution to the restoring force in the

unstrained crystal

$$F(0, z) = 12\alpha'_0 z \quad (A4a)$$

and hence

$$U(0, z) = 6\alpha'_0 z^2. \quad (A4b)$$

When the stress is applied the bond vectors change to

$$\begin{aligned}\vec{r}_1 &= (\tfrac{1}{4}a_0)(1 - \epsilon, 1 - \epsilon, 3 + 6\epsilon), \\ \vec{r}_2 &= (\tfrac{1}{4}a_0)(3 - 3\epsilon, 1 - \epsilon, 1 + 2\epsilon),\end{aligned} \quad (A5)$$

and relevant angles can be computed using

$$\cos\theta_i = \hat{r}_i \cdot \hat{n}, \quad (A6)$$

where  $\hat{r}_i$  and  $\hat{n}$  are unit vectors in the direction of the bond  $\vec{r}_i$  and the stress axis, respectively. Using Eqs. (A2), (A5), and (A6) we find in the strained crystal

$$U(\epsilon, z) = 6\alpha'_0 [1 + 4\epsilon g(n')] z^2, \quad (A7)$$

where

$$g(n') = 1 + \tfrac{1}{2} \left(\tfrac{8}{11}\right)^2 (n' - 2) \quad (A8)$$

and

$$n' = \left. \frac{d(\ln\alpha')}{d(\ln r)} \right|_{r=r_0}. \quad (A9)$$

Assuming  $n' = n$  the total effective force constant in the presence of the strain is given by Eq. (55).

## 2. [111] Stress

For this stress direction only three bond vectors need be considered:  $\vec{r}_1$ ,  $\vec{r}_2$ , and  $\vec{r}_3$ . These bond vectors for the unstrained crystal are given by Eq. (A1), and for the crystal subject to a strain as described by the strain tensor of Eq. (39) they are

$$\begin{aligned}\vec{r}_1 &= (\tfrac{1}{4}a_0)(1 + 4\epsilon - 2\epsilon\zeta, 1 + 4\epsilon - 2\epsilon\zeta, 3 + 2\epsilon - 2\epsilon\zeta), \\ \vec{r}_2 &= (\tfrac{1}{4}a_0)(-1 + 2\epsilon\zeta, -1 + 2\epsilon - 2\epsilon\zeta, 3 - 2\epsilon - 2\epsilon\zeta), \\ \vec{r}_3 &= (\tfrac{1}{4}a_0)(-3 - 2\epsilon\zeta, -1 - 2\epsilon - 2\epsilon\zeta, 1 - 4\epsilon - 2\epsilon\zeta).\end{aligned} \quad (A10)$$

Proceeding in the same way as before we obtain the third neighbor contribution to the bond-stretching energy in the presence of strain:

$$U(\epsilon, z) = 6\alpha'_0 [1 + 4\epsilon h(n, \zeta)] z^2, \quad (A11)$$

where  $h(n, \zeta)$  is given by Eq. (60) and we again assume  $n' = n$ .

\*Supported by Army Research Office, Durham; the National Science Foundation; and the Advanced Research Projects Agency.

<sup>1</sup>See, for example, F. H. Pollak in *Proceedings of the Tenth International Conference on the Physics of Semiconductors*, Cambridge, 1970 (U.S. Atomic Energy Com-

mission, Oak Ridge, Tenn., 1970), p. 407.

<sup>2</sup>E. Anastassakis, A. Pinczuk, E. Burstein, F. H. Pollak, and M. Cardona, *Solid State Commun.* **8**, 133 (1970).

<sup>3</sup>Y. D. Harker, C. Y. She, and D. F. Edwards, *Appl. Phys. Letters* **15**, 272 (1969).

- <sup>4</sup>W. J. Burke, R. J. Pressley, and J. C. Slonczewski, *Solid State Commun.* **9**, 121 (1971).
- <sup>5</sup>F. Cerdeira, C. J. Buchenauer, F. H. Pollak, and M. Cardona, *Bull. Am. Phys. Soc.* **16**, 29 (1971).
- <sup>6</sup>S. Ganesan, A. A. Maradudin, and J. Oitmaa, *Ann. Phys. (N.Y.)* **56**, 556 (1970).
- <sup>7</sup>R. M. Martin, *Phys. Rev. B* **1**, 4005 (1970).
- <sup>8</sup>M. J. P. Musgrave and J. A. Pople, *Proc. Roy. Soc. (London)* **A268**, 974 (1962).
- <sup>9</sup>H. L. McMurray, A. W. Solbrig, Jr., J. K. Boyter, and C. Noble, *J. Phys. Chem. Solids* **28**, 2359 (1967).
- <sup>10</sup>A. W. Solbrig, Jr., Idaho Nuclear Corporation Report No. IN-1424, 1970 (unpublished).
- <sup>11</sup>S. S. Mitra, O. Brafman, W. B. Daniels, and R. K. Crawford, *Phys. Rev.* **186**, 942 (1970).
- <sup>12</sup>J. Buchenauer, F. Cerdeira, and M. Cardona, International Conference of Light Scattering in Solids, Paris, 1971 (unpublished).
- <sup>13</sup>In the case of ZnSe the Raman scattering is from the bulk of the material since it is transparent to the incident and scattered radiation and therefore the scattering is not sensitive to the surface treatment.
- <sup>14</sup>R. Loudon, *Advan. Phys.* **13**, 423 (1964).
- <sup>15</sup>B. Weinstein (private communication).
- <sup>16</sup>S. Ganesan and A. A. Maradudin (private communication).
- <sup>17</sup>See, for example, L. Kleinman, *Phys. Rev.* **128**, 2614 (1962).
- <sup>18</sup>A. Segmuller and H.R. Neyer, *Physik Kondensierten Materie* **4**, 63 (1965).
- <sup>19</sup>F. Herman, *J. Phys. Chem. Solids* **8**, 405 (1959).
- <sup>20</sup>K. Kunc, M. Balkanski, and M. Nusimovici, *Phys. Status Solidi* **41**, 491 (1970).